© 2014. Published by The Company of Biologists Ltd | Development (2014) 141, 4729-4739 doi:10.1242/dev.108092

RESEARCH ARTICLE

Oncogenic Ras stimulates Eiger/TNF exocytosis to promote growth

Chiswili Chabu and Tian Xu*

ABSTRACT

Oncogenic mutations in Ras deregulate cell death and proliferation to cause cancer in a significant number of patients. Although normal Ras signaling during development has been well elucidated in multiple organisms, it is less clear how oncogenic Ras exerts its effects. Furthermore, cancers with oncogenic Ras mutations are aggressive and generally resistant to targeted therapies or chemotherapy. We identified the exocytosis component Sec15 as a synthetic suppressor of oncogenic Ras in an *in vivo Drosophila* mosaic screen. We found that oncogenic Ras elevates exocytosis and promotes the export of the pro-apoptotic ligand Eiger (*Drosophila* TNF). This blocks tumor cell death and stimulates overgrowth by activating the JNK-JAK-STAT non-autonomous proliferation signal from the neighboring wild-type cells. Inhibition of Eiger/TNF exocytosis or interfering with the JNK-JAK-STAT non-autonomous proliferation signaling at various steps suppresses oncogenic Ras-mediated overgrowth. Our findings highlight important cell-intrinsic and cell-extrinsic roles of exocytosis during oncogenic growth and provide a new class of synthetic suppressors for targeted therapy approaches.

KEY WORDS: Eiger, TNF, Exocytosis, Oncogenic Ras, Tumors

INTRODUCTION

Activating mutations of the oncogenic Ras gene are highly prevalent in human cancers (Bos, 1989). However, targeted therapy strategies have not yielded the desired effects and the available chemotherapy regimens are not effective at treating the most aggressive Ras cancers (Asghar et al., 2010; Lièvre et al., 2010). Genetic studies in fruit flies and worms have led to the identification of Ras effectors and the characterization of the Ras/Raf/mitogen activated protein kinases (Ras/MAPK) signaling cascade during normal development (Nishida and Gotoh, 1993; Simon et al., 1991; Sternberg and Horvitz, 1991). This pathway was found to be conserved in mammals (Alessi et al., 1994; Cowley et al., 1994; Kolch et al., 1991; Mansour et al., 1994; Qiu et al., 1995). However, targeting components of the Ras/MAPK signaling cascade only partly inhibits overgrowth (Blum and Kloog, 2005), suggesting that oncogenic Ras drives tumorigenesis via additional signaling events. Moreover, blocking the Ras/MAPK pathway causes death of normal cells, thus making this approach not suitable for targeted therapy and placing an impetus on the need to identify the additional signaling events that oncogenic Ras specifically triggers to promote tumor development. Identification of mutations that synthetically suppress Ras tumor growth could not only broaden our understanding of cancer biology, but could also lead to the discovery of novel therapeutic targets. Indeed, several laboratories have conducted RNA interference (RNAi)-based synthetic suppressor screens in tissue culture settings and have identified important vulnerabilities of oncogenic Ras cells (Barbie et al., 2009; Luo et al., 2009; Sarthy et al., 2007; Scholl et al., 2009; Steckel et al., 2012; Strebhardt and Ullrich, 2006). Additional whole-animal synthetic suppressor screens could be particularly informative for revealing the role of oncogenic Ras in processes that are important for regulating growth *in vivo*.

Expression of oncogenic Ras (Ras^{V12}) in *Drosophila* imaginal discs gives rise to overgrowth (Karim and Rubin, 1998). Generating patches of labeled Ras^{V12}-expressing cells surrounded by wild-type cells allows putative host-tumor cell interactions to occur and permits genetic screens to identify mutations that can either enhance or suppress the growth of Ras^{V12}-expressing tumors (Chi et al., 2010; Pagliarini and Xu, 2003). Here, we report the characterization of one of the synthetic suppressor mutations, *sec15*, a mutation in a gene that encodes a component of the exocytosis machinery. Sec15 is a subunit of the evolutionarily conserved multiprotein complex termed the Sec6/Sec8 complex or the exocyst complex, which was originally identified in yeast (Finger et al., 1998; Finger and Novick, 1998; Guo et al., 1999; Heider and Munson, 2012; Novick et al., 1980; TerBush and Novick, 1995). The exocyst complex regulates secretion in eukaryotes by controlling the delivery of vesicles to the cell plasma membrane (Grindstaff et al., 1998; Guo et al., 1999; Heider and Munson, 2012; Jafar-Nejad et al., 2005; Mehta et al., 2005; TerBush and Novick, 1995). In contrast to core exocyst components, which are broadly required for normal exocyst function and cell viability, Sec15 regulates the delivery of specific cargo proteins and is dispensable for cell viability in *Drosophila* (Mehta et al., 2005).

In addition to being essential for cellular organization in all eukaryotes, vesicle transport has recently been found to play important roles in regulating signal transduction. For example, transport of endocytosed cell surface molecules to signaling targets on endosomes allows signal transduction to occur, whereas targeting these molecules to the lysosome for degradation attenuates or suppresses signaling (Seto et al., 2002). Transcytosis of vesicles facilitates the establishment of morphogen gradients, which are crucial for conveying proliferation and cell fate specification cues during development (Seto et al., 2002). Exocytosis has been previously found to mediate signal transduction by sending signaling molecules including neurotransmitters and ligands to neighboring cells (Li and Chin, 2003). By studying how *sec15* suppresses Ras^{V12}, we show that exocytosis also regulates signal transduction within a cell by clearing signaling ligands. We found that Ras^{V12} cells clear Eiger (also known as TNF) by exocytosis to downregulate pro-apoptotic Janus NH2-terminal kinase (JNK, also known as Bsk – FlyBase) signaling (Igaki et al., 2009; Moreno et al., 2002) and thus evade cell death. We have previously shown that JNK activation triggered by cell polarity defects could stimulate non-autonomous JAK-STAT signaling for proliferation (Wu et al., 2010).

Department of Genetics, Howard Hughes Medical Institute, Yale University School of Medicine, Boyer Center for Molecular Medicine, 295 Congress Avenue, New Haven, CT 06536, USA.

*Author for correspondence (tian.xu@yale.edu)

Received 17 January 2014; Accepted 7 October 2014

Development (2014) 141, 4729-4739 doi:10.1242/dev.108092

Here, we show that oncogenic Ras elevates exocytosis to hijack this process in order to promote overgrowth. Exocytosis-dependent accumulation of Eiger/TNF results in JNK activation in surrounding wild-type cells, which in turn, non-autonomously stimulates JAK-STAT signaling to promote the proliferation of Ras^{V12} cells. These findings provide new mechanistic insights into the long known ability of oncogenic Ras cells to avoid cell death and promote growth, and also highlight the importance of exocytosis in signal transduction and cancer biology.

RESULTS

sec15 synthetically interacts with oncogenic Ras

In *Drosophila*, GFP-marked mosaic clones of cells expressing Ras^{V12} overgrow to develop into tumors (Pagliarini and Xu, 2003). The overgrowth phenotype can be readily ascertained by visualizing fluorescent signal intensity in third instar whole larvae (Fig. 1A,C) or by examining clone size in dissected eye-antenna imaginal discs (Fig. 1E,G). Furthermore, Ras^{V12} tumors caused pupal lethality (98.4%, *N*=62; Fig. 1K). We induced *sec15* or Ras^{V12} single mutant clones or Ras^{V12}, *sec15* double mutant clones and examined the growth of these mutant clones in similarly aged third instar eye-antenna discs. We found that the *sec15* mutation did not disrupt cell proliferation (supplementary material Fig. S1A,B), and the size of *sec15* mutant clones was comparable to that of wild-type clones (Fig. 1A,B,E,F), consistent with the reported cell viability of the *sec15* null mutation (Mehta et al., 2005). In addition, *sec15* null mutant cells persisted into the adult eye (Fig. 1I,J). The viability of *sec15* mutant cells is not due to maternal protein deposition, as Sec15 protein level was dramatically reduced in mutant clone cells (supplementary material Fig. S2A). However, the *sec15* mutation dramatically suppressed the overgrowth phenotype of Ras^{V12} clones (Fig. 1C,D,G,H; 77.4% of the double mutants showed strong suppression similar to that shown in Fig. 1D,H; *N*=53). Furthermore, the *sec15* mutation rescued the lethality of the animals bearing Ras^{V12} tumors (76% viable, *N*=125, compared with 1.6% viable, *N*=62 for Ras^{V12} animals; Fig. 1L). Moreover, RNA interference (RNAi)-mediated knockdown of *Sec15* in Ras^{V12}, $scrib^{-}$ cells suppressed tumor growth and invasion (supplementary material Fig. S8A-D). Finally RNAi knockdown of two core exocyst components, *Sec6* and *Sec8* showed a similar effect on Ras^{V12}-mediated overgrowth (supplementary material Fig. S1C-N). The *sec15* mutant or *Sec15* or *Sec8* RNAi alone had no detectable effect on growth, whereas *Sec6* RNAi alone showed a reduction in clone sizes (supplementary material Fig. S1C-N). Taken together, we conclude that the *sec15* mutation synthetically suppresses Ras^{V12} tumor growth.

Oncogenic Ras stimulates the exocyst

Interestingly, it was previously observed that RNAi depletion of exocytosis proteins also suppresses $HRas^{V12}$-mediated tumor growth in human cells (Issaq et al., 2010). We thus investigated the mechanism underlying this phenomenon. The observation that *sec15* can selectively suppress Ras^{V12} tumor growth suggested that oncogenic Ras could regulate the exocyst to promote growth. We first analyzed the abundance of exocyst proteins in Ras^{V12} tumor clones relative to that of wild-type cells. We examined Sec15 protein levels in Ras^{V12} tumors and extended this analysis to include Sec6, Sec8 and Rab11. Rab11 interacts with Sec15 to initiate assembly of the exocyst and the exocytosis of endocytosed molecules (Wu et al., 2005; Zhang et al., 2004). The previously published Sec15, Sec6 and Sec8 antibodies showed negligible staining in corresponding mutant and RNAi knockdown clones (supplementary material Fig. S2A-C). Sec15, Sec6 and Sec8 proteins were specifically upregulated in Ras^{V12}clones (Fig. 2A-C,E,G). Similarly, Rab11 was upregulated in Ras^{V12} cells (Fig. 2D,F). The increased levels of exocyst proteins in Ras^{V12} cells were subsequently confirmed by western blotting (Fig. 2H). Exocyst proteins displayed no obvious subcellular localization defects in Ras^{V12} cells (Fig. 2E-G), indicating that oncogenic Ras stimulates exocyst proteins but does not affect their respective subcellular localization.

The observation that Rab11 is upregulated along with core exocyst proteins suggested that oncogenic Ras elevates the secretion of endocytosed molecules. To begin to address this possibility, we sought to examine the transport of endocytosed molecules in the mutant cells by performing Dextran dye pulse-chase experiments. After the dye pulse phase we found that Ras^{V12} cells had no problem

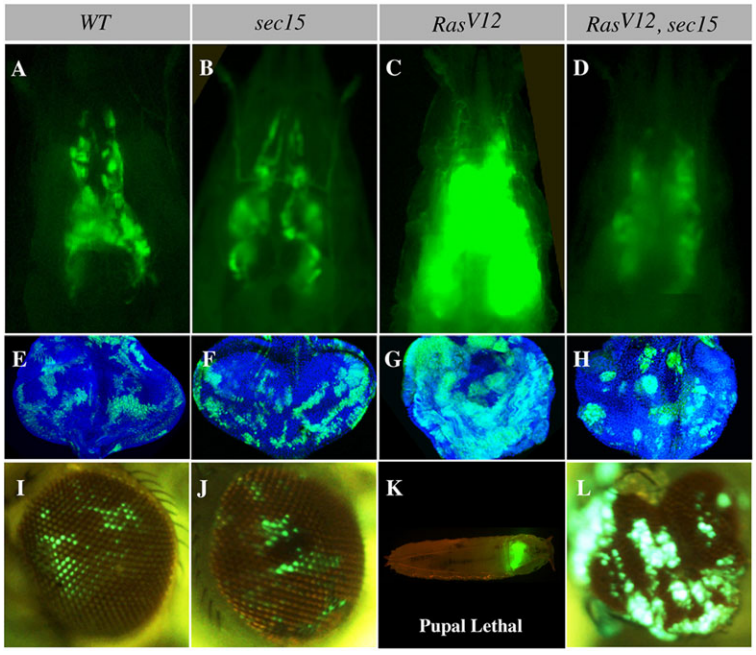

Fig. 1. Ras^{V12} and *sec15* synthetic lethal interaction. (A-D) Intact third instar larval cephalic regions showing wild-type (WT), *sec15*, Ras^{V12} and Ras^{V12}, *sec15* double mutant eye-antenna disc clones. Wild-type (A) and *sec15* (B) clones are comparable in size, whereas Ras^{V12} clones (C) overgrow to develop tumors. The *sec15* mutation suppresses Ras^{V12} tumor growth (D). (E-H) Similarly aged eye discs bearing wild-type, *sec15*, Ras^{V12} and Ras^{V12}, *sec15* double mutant clones. Wild-type (E) and *sec15* (F) clones show a comparable sparse pattern, whereas Ras^{V12} clones (G) overgrow to form large contiguous tumors. However, Ras^{V12}, *sec15* double mutant clones are sparse and smaller (H). (I-L) Adult eyes showing lethality and contribution of larval clones to the eye field. Wild-type (I) and *sec15* (J) clones similarly persist into the adult eye and do not cause animal lethality. Ras^{V12} clones (K) are pupal lethal but animal lethality is suppressed in animals bearing Ras^{V12}, *sec15* double mutant clones, and cells of this genotype now contribute to the adult eye (L).

Development (2014) 141, 4729-4739 doi:10.1242/dev.108092

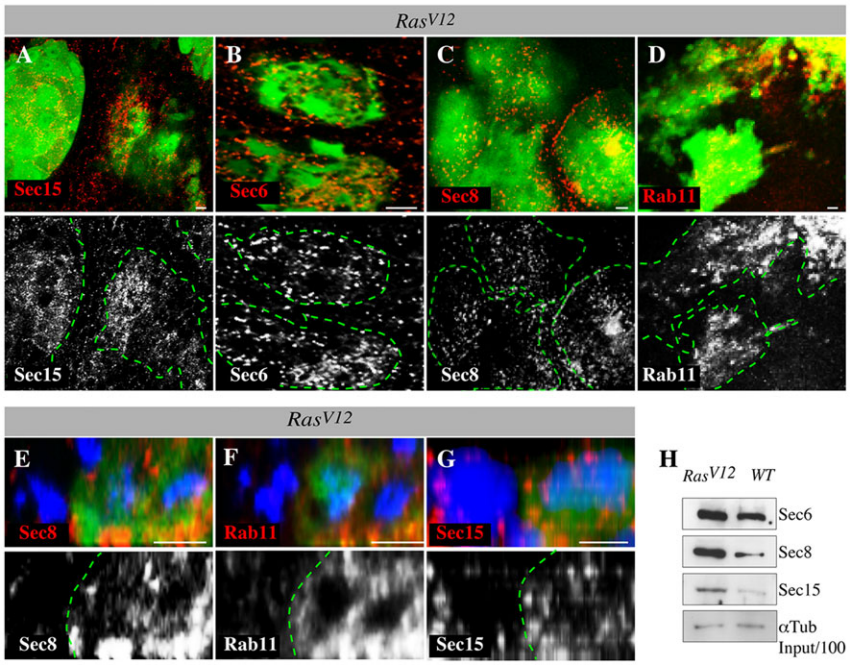

Fig. 2. *Ras^{V12}* cells upregulate exocyst proteins. (A-G) *Ras^{V12}* clones stained with antibodies against exocyst proteins (Sec15, Sec6, Sec8 and Rab11) and co-stained with DAPI (blue) to mark nuclei. Lower panels show Sec15, Sec6, Sec8 and Rab11 channels alone. Sec15 is upregulated in *Ras^{V12}* cells (A). Similarly, Sec6 (B), Sec8 (C) and Rab11 (D) are upregulated in *Ras^{V12}* clones but not in neighboring wild-type cells. Green dotted lines denote clone boundaries. (E-G) *x*/*z* confocal projection images of *Ras^{V12}* clones (green) stained with anti-Sec8, anti-Rab11 and anti-Sec15, and with DAPI. Sec8 (E), Rab11 (F) and Sec15 (G) proteins display no obvious localization defects but show increased abundance in *Ras^{V12}* cells. (H) Lysate from discs bearing wild-type (WT) or *Ras^{V12}* clones immunoblotted with anti-Sec6, anti-Sec8, anti-Sec15 or anti-Tubulin antibodies (loading control). Sec6, Sec8 and Sec15 protein abundance is increased in *Ras^{V12}* lysates.

taking up the dye as they contained more dye (dye-positive punctae) than control cells [4.05±1.47 for *Ras^{V12}* versus 2.29±0.65 for wild-type cells (means±s.d.); Fig. 3A,B,G], indicating that endocytosis is generally not inhibited in *Ras^{V12}* cells. Examining dye abundance in mutant versus control cells after the dye chase period provided a crude measure of secretion within these cells. Interestingly, *Ras^{V12}* cells were significantly more efficient at dye clearance after the dye chase phase. *Ras^{V12}* cells showed fewer dye-positive punctae compared with wild-type cells (the pulse:chase ratios of dye-positive punctae for *Ras^{V12}* and wild-type cells were 4.63±0.27 and 1.53±1.12, respectively; Fig. 3D,E,G). The *sec15* mutation abrogated the increased dye clearance effect of oncogenic Ras [2.74±1.98 (after the pulse), 1.26±0.29 (after chase) and 2.18±0.34 (pulse:chase ratio); Fig. 3C,F,G]. Taken together, the above data indicate that oncogenic Ras stimulates the exocyst.

Oncogenic Ras promotes the interaction of Eiger/TNF with the exocyst

We next sought to investigate the significance of exocyst stimulation vis-à-vis tumor growth. One way in which Ras activation contributes to tumorigenesis is by allowing the cell to evade cell death (Cox and Der, 2003; Downward, 1998; Wolfman et al., 2002; Wu et al., 2009). In *Drosophila*, the tumor necrosis factor (TNFα) homolog Eiger triggers cell death (Igaki et al., 2009; Moreno et al., 2002). Similar to vertebrate TNFs, Eiger is produced as a transmembrane protein and is subsequently cleaved to yield a soluble ligand (Black et al., 1997; Brandt et al., 2004; Jue et al., 1990; Kauppila et al., 2003; Moss et al., 1997). Eiger/TNF is endocytosed to activate JNK signaling on endosomes, which triggers cell death (Igaki et al., 2009; Moreno et al., 2002). Preventing endocytosis impinges on Eiger/TNF signaling (Igaki et al., 2009). Because endocytosis is not generally inhibited in *Ras^{V12}* cells and *sec15* suppresses oncogenic Ras-mediated overgrowth, we hypothesized that oncogenic Ras could promote an interaction between the exocyst and Eiger/TNF in order to accelerate cellular clearance of Eiger/TNF, hence preventing Eiger/TNF signaling from directly killing tumor cells. We first examined whether Eiger/TNF and Sec15 proteins interact in *Ras^{V12}* cells using two independent and complementary approaches, immunostaining and biochemistry. We found that Eiger/TNF colocalized with Sec15 in *Ras^{V12}* cells (Fig. 4A-C). Sectioning of isosurface-rendered images from confocal projections revealed that indeed Sec15 coats Eiger/TNF-positive vesicles (Fig. 4D), suggesting that Eiger/TNF is a Sec15 cargo protein. Moreover, we performed anti-Eiger or anti-GFP control pulldown experiments on lysate prepared from eye-antenna discs bearing *Ras^{V12}* clones and found that Sec15 and other exocyst proteins, Sec5 and Sec8, specifically co-precipitated with Eiger/TNF (Fig. 4M). We conclude that oncogenic Ras promotes the interaction of the exocyst with Eiger/TNF.

Oncogenic Ras promotes Eiger/TNF exocytosis to prevent tumor cell death

Endocytosed molecules destined for secretion are shuttled to the cell cortex in Rab11-positive endosomes (Dollar et al., 2002; Sonnichsen et al., 2000; Ullrich et al., 1996). We thus tested whether Eiger/TNF localizes to early (Rab5-positive) endosomes and to recycling (Rab11-positive) endosomes. We found that Eiger/TNF colocalized with both Rab5 and Rab11 endosomes (Fig. 4E-L). Together with the Eiger/TNF-exocyst interaction data above, these observations supported the notion that Eiger/TNF is being cleared out of *Ras^{V12}* tumors by exocytosis. To directly test this, we examined Eiger/TNF protein distribution in similarly aged *Ras^{V12}* or *Ras^{V12}*, *sec15* mutant clones. We found that Eiger/TNF accumulated at the margins of *Ras^{V12}* clones (Fig. 5A-C), consistent with the Eiger/TNF protein being exocytosed.

Importantly, examination of *Ras^{V12}*, *sec15* double mutant clones revealed that Eiger/TNF no longer accumulated at the boundary, but rather accumulated within the clones (Fig. 5D,E). The *sec15* mutant clones showed a moderate retention of Eiger/TNF (Fig. 5V,W). We then depleted Eiger/TNF specifically in the *Ras^{V12}* cells and found that this prevented the accumulation of Eiger/TNF that is otherwise seen as a ring around the clones (Fig. 5F,G).

Furthermore, the cellular release of soluble TNF from its precursor transmembrane form and its resulting activity are mediated by the TNF-converting enzyme, Tace (Black et al., 1997; Blobel, 1997; Moss et al., 1997). Eiger/TNF contains a Tace cleavage site

Development (2014) 141, 4729-4739 doi:10.1242/dev.108092

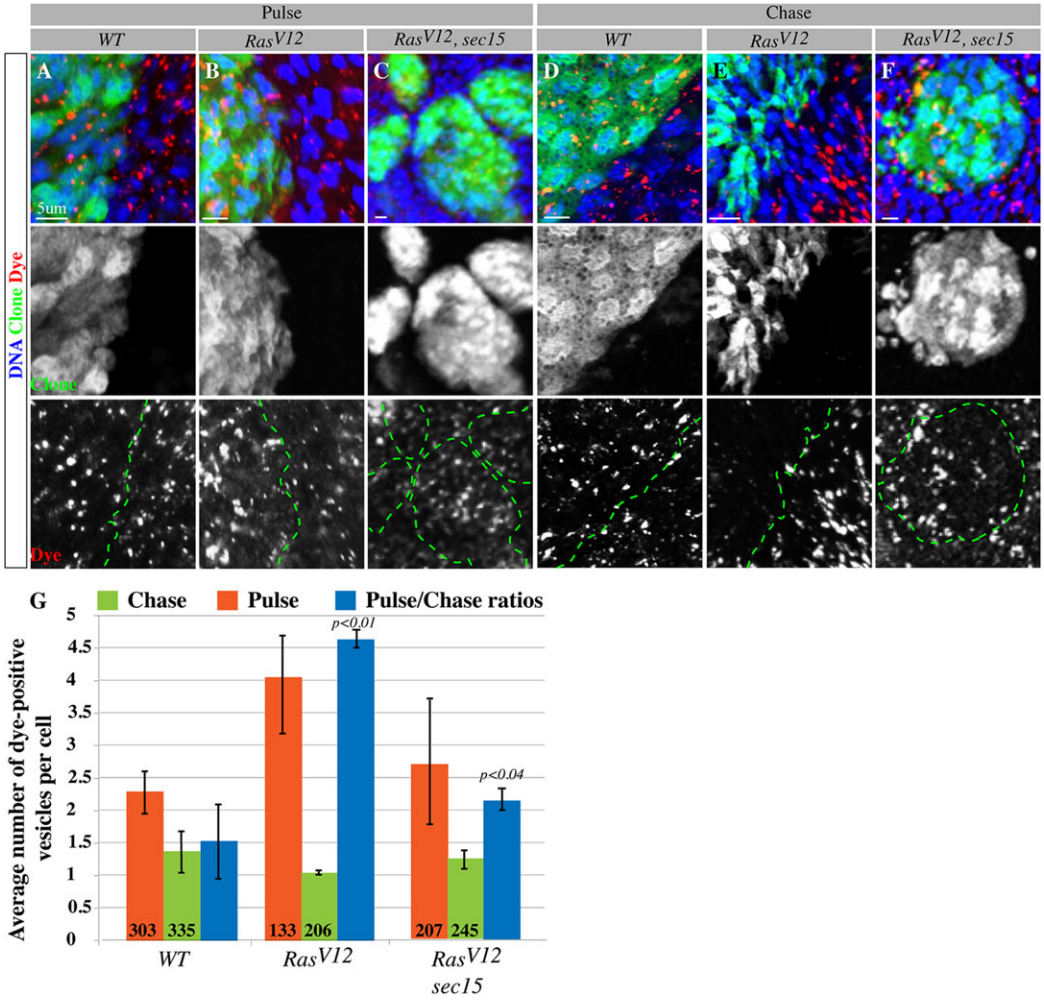

Fig. 3. *Ras^{V12}* cells stimulate secretion through Sec15. (A-F) Projections of confocal images showing wild-type (WT), *Ras^{V12}* or *Ras^{V12}, sec15* mutant clones (green, middle panels) after pulse (A-C) and followed by a chase period (D-F) of Dextran dye (red, lower panels). Samples are co-stained with DAPI (blue) to mark nuclei. Middle panels show the clone channel alone. The dotted green lines in the lower panels denote clone boundaries. *Ras^{V12}* cells (B) show no problem in dye uptake. Cellular clearance of the dye is accelerated in *Ras^{V12}* cells (E, lower panel) compared with that of similarly treated wild-type control cells (D, lower panel). The *sec15* mutation suppresses the ability of *Ras^{V12}* cells to clear out the dye (C,F). (G) Quantification of A-F. The number of dye-positive vesicles after each experimental phase (pulse and chase) was scored in multiple clones for each genotype. Pulse:chase ratios were derived from averages of dye-positive vesicle numbers after each experimental phase. Error bars represent standard deviation from the mean for each genotype analyzed. In this and all subsequent figures, numbers within bars indicate the number of cells analyzed per corresponding genotype.

equivalent to TNFα cleavage site in vertebrates (Kauppila et al., 2003; Narasimamurthy et al., 2009). We first verified that *Drosophila* Tace plays a similar role in Eiger/TNF signaling. First, we found that RNAi knockdown of the sole *Drosophila* Tace in the developing eye suppressed the Eiger/TNF-mediated small-eye phenotype (supplementary material Fig. S3A-D). Similar results were obtained in wing imaginal discs (data not shown). We subsequently tested for a role for Tace in Eiger/TNF non-autonomous signaling using the hanging-eye phenotype model (Narasimamurthy et al., 2009). We found that coexpression of *eiger* and *Tace* in cells rescued by expression of the dominant-negative JNK allele *bsk-DN* in the developing eye (*GMR>egr*,*Tace*,*bsk-DN*) produced a hanging-eye phenotype (supplementary material Fig. S3F,F′). The majority of *GMR>egr*,*Tace*,*bsk-DN* animals die in late pupal stages (73%, *N*=157) and show a ring of necrotic tissue around the eyes (supplementary material Fig. S3F″). Interestingly, the *GMR>egr*,*bsk-DN* animals did not have a dramatic hanging-eye phenotype (supplementary material Fig. S3E). These data indicate that Tace plays an important role in the secretion and signaling of Eiger. Finally, we knocked down Tace by RNAi in the *Ras^{V12}* cells and found that this abolished Eiger/TNF accumulation around the *Ras^{V12}* clones (supplementary material Fig. S4). Collectively, these data indicate that the pool of Eiger/TNF seen around *Ras^{V12}* clones originates from *Ras^{V12}* cells, and Sec15 plays an important role in Eiger/TNF protein export.

Eiger/TNF normally activates JNK signaling to trigger cell death (Igaki et al., 2009; Moreno et al., 2002). Correspondingly, we found that JNK activity was elevated inside the *Ras^{V12}*, *sec15* double mutant clones compared with that of *Ras^{V12}* or *sec15* mutant clones (Fig. 5H,L,X,Y). Increased JNK signaling correlated with increased ectopic cell death inside the *Ras^{V12}*, *sec15* double mutant clones compared with *Ras^{V12}* single mutant clones, as measured by activated caspase-3 immunoreactivity, a cell death indicator (58.74±19.48%; *N*=257 versus 6.99±4.32%; *N*=699 caspase-positive cells, respectively; mean±s.d.; Fig. 5O-Q versus Fig. 5R,S; Fig. 5Z). Furthermore, concomitant suppression of JNK signaling, by expressing the dominant-negative JNK allele *bsk-DN*, restored viability to *Ras^{V12}*, *sec15* clones (3.85±5.8%; *N*=408 caspase-

Development (2014) 141, 4729-4739 doi:10.1242/dev.108092

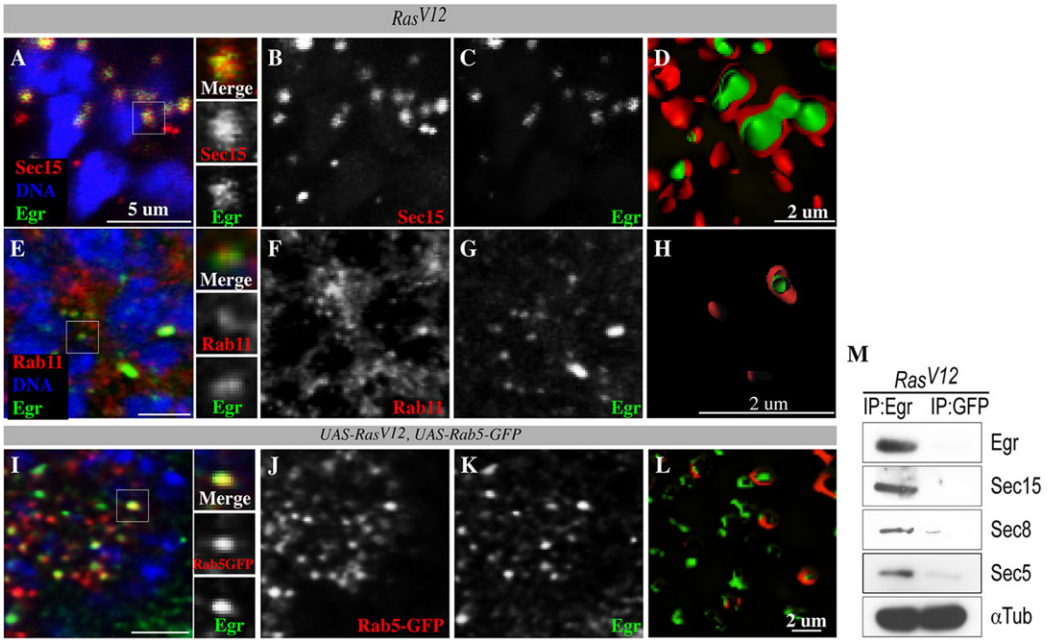

Fig. 4. Sec15 interacts with Eiger/TNF. (A-D) *Ras*^{V12} cells counterstained with anti-Sec15 (red) and anti-Eiger (green). Sec15 and Eiger colocalize (A; side panels represent magnified view from white box). B and C are single channels for Sec15 and Eiger from A. (D) Cross-section images of isosurface-rendered confocal projection images showing Eiger (green) inside Sec15-coated (red) vesicles. (E-H) *Ras*^{V12} cells counterstained with anti-Rab11 (red) and anti-Eiger (green). Rab11 and Eiger colocalize (E; side panels represent magnified view from white box). F and G are single channels for Rab11 and Eiger from E. (H) Cross-section of isosurface-rendered confocal projection showing Eiger (green) inside Rab11-coated (red) vesicles. (I-L) *Ras*^{V12} cells co-expressing Rab5-GFP (red) counterstained with anti-Eiger (green). Rab5-GFP and Eiger colocalize (I; side panels represent magnified view from white box). J and K are single channels for Rab5-GFP and Eiger, respectively. (L) Cross-section of isosurface-rendered confocal projections showing Eiger (green) inside Rab5-GFP-coated (red) vesicles. (M) Anti-Eiger or anti-GFP (control) immunoprecipitation experiments with lysate derived from tissues bearing *Ras*^{V12} clones. Immunoprecipitates (IP) were blotted with antibodies against Sec15, Sec8, Sec5 and α-Tubulin (loading control).

positive cells; Fig. 5T,U,Z). We conclude that Sec15-dependent exocytosis of Eiger/TNF downregulates JNK to protect *Ras*^{V12} cells from apoptosis.

Eiger/TNF activates JAK-STAT signaling non-autonomously

Although blocking JNK signaling in *Ras*^{V12}, *sec15* double mutant clones suppresses cell death, it fails to fully restore *Ras*^{V12} tumor growth (supplementary material Fig. S5A,B). This suggests that Sec15 contributes to *Ras*^{V12} tumor growth by an additional mechanism. Similar to vertebrate TNF, Eiger can act non-autonomously (Cordero et al., 2010; Pérez-Garijo et al., 2013). In addition, it has been shown that JNK signaling can non-autonomously stimulate the proliferation of adjacent cells (Ryoo et al., 2004; Wu et al., 2010), thus we wondered whether the Sec15-dependent accumulation of Eiger/TNF in the surrounding wild-type cells activates JNK to promote *Ras*^{V12} tumor growth. We tested whether JNK is activated in the wild-type cells surrounding *Ras*^{V12} clones. JNK activity was elevated in wild-type cells surrounding *Ras*^{V12}tumors (Fig. 5H-J), but not in wild-type cells surrounding the Eiger/TNF-secretion-defective *Ras*^{V12}, *sec15* double mutant clones or the Eiger/TNF RNAi-depleted *Ras*^{V12} clones (Fig. 5K-N). In agreement with this and previous findings (Karim and Rubin, 1998), we could detect activated caspase-positive cells around *Ras*^{V12} tumors (Fig. 5O-Q). Therefore, increased Eiger/TNF secretion by *Ras*^{V12} cells leads to Eiger/TNF accumulation and activation of JNK signaling in surrounding wild-type cells. This is consistent with earlier reports of Eiger/TNF activating JNK non-autonomously (Cordero et al., 2010; Pérez-Garijo et al., 2013).

We have previously shown that JNK activation triggered by cell polarity defects can induce the expression of JAK-STAT ligands encoded by the *unpaired* (*upd*) genes. Upd ligands cooperate with *Ras*^{V12} through non-autonomous JAK-STAT activation (Wu et al., 2010). Blocking JNK signaling in *Ras*^{V12} cells has no obvious effect on their proliferation (Igaki et al., 2006), supporting the possibility that the observed JNK activation in surrounding wild-type cells could promote *Ras*^{V12} tumor growth by a non-cell autonomous mechanism. We thus wondered whether Eiger/TNF-exocytosis-mediated JNK activation in the surrounding cells promotes the growth of *Ras*^{V12} cells. We first examined Upd expression levels using the Upd-lacZ reporter line (Sun et al., 1995) and found that Upd was particularly up-regulated in wild-type cells surrounding *Ras*^{V12} clones (supplementary material Fig. S6D). Next, we used a JAK-STAT activity GFP reporter (Bach et al., 2007), which includes the promoter fragment of *Socs36E*, a transcriptional target of JAK-STAT signaling (Karsten et al., 2002), to examine JAK-STAT activity level in *Ras*^{V12} cells. JAK-STAT was upregulated in *Ras*^{V12} cells and in the surrounding Upd-producing wild-type cells (Fig. 6A). This increase was more robust in larger *Ras*^{V12} clones than in smaller ones (supplementary material Fig. S6B, arrow versus boxed area). Similarly, Stat92E immunoreactivity, which is an indicator of JAK-STAT pathway activation (Chen et al., 2002; Johansen et al., 2003), was elevated in *Ras*^{V12} discs (supplementary material Fig. S6F). In a complementary experiment, we found that the transcription level of *Socs36E* was elevated in *Ras*^{V12} discs compared with that of wild-type control discs (Fig. 6F), consistent with the STAT-GFP and Stat92E results. This indicates that JAK-STAT signaling is activated in *Ras*^{V12} cells.

To test whether the observed activation of JAK-STAT in *Ras*^{V12} cells is due to increased Eiger/TNF exocytosis to neighboring wild-

Development (2014) 141, 4729-4739 doi:10.1242/dev.108092

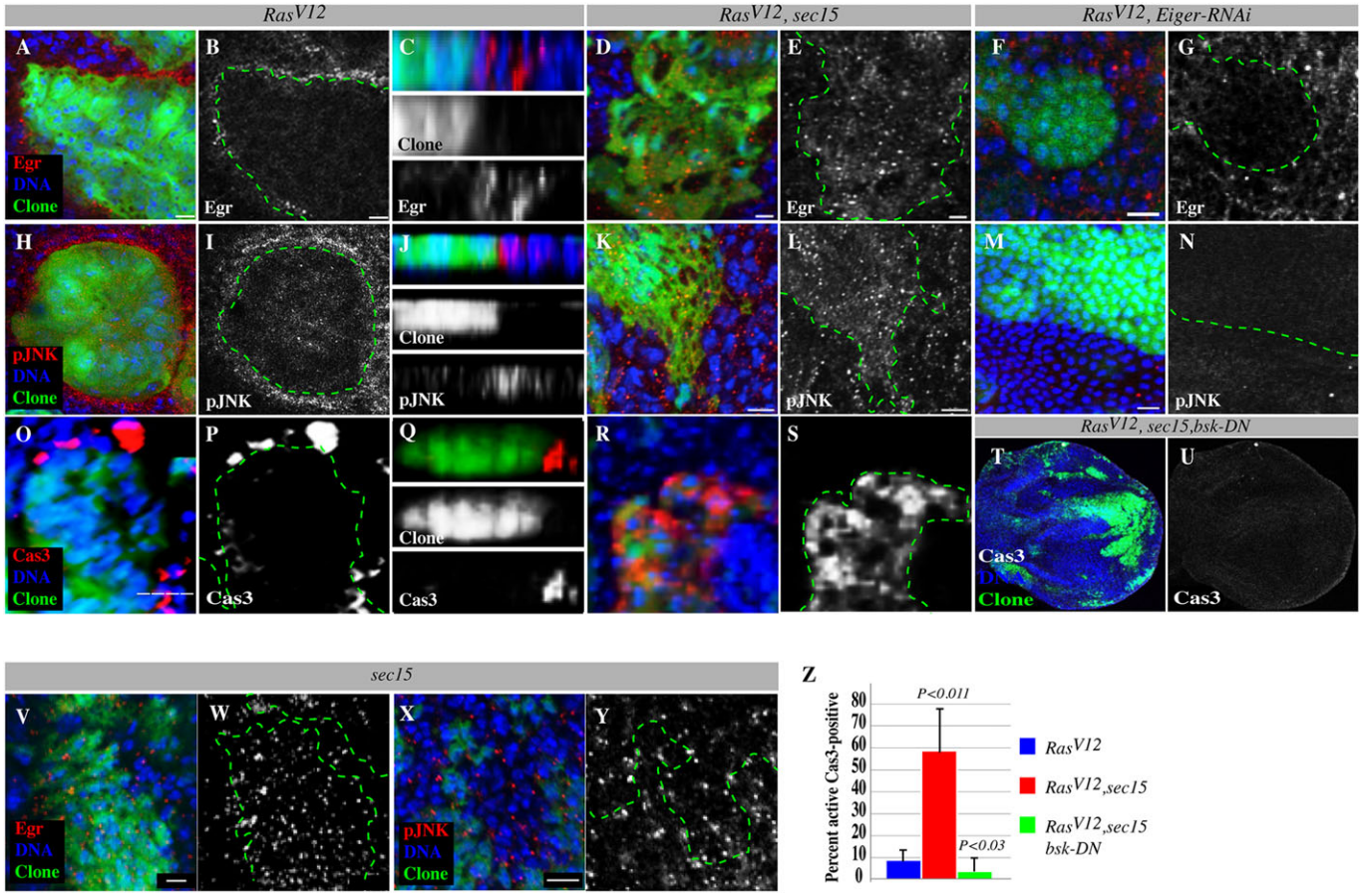

Fig. 5. Sec15-dependent Eiger exocytosis suppresses JNK-induced cell death in Ras^{V12} cells but promotes JNK activation in the surrounding wild-type cells. (A-Y) Comparable *z*-sections showing Ras^{V12} or Ras^{V12}, *sec15* double mutant clones or Ras^{V12}, *eiger-RNAi* clones (green) stained with anti-Eiger (red) or anti-phospho-JNK (pJNK, red) to detect JNK signaling activity or anti-active caspase 3 to detect apoptotic cells, and with DAPI (blue) to mark DNA. Gray panels show Eiger, phospho-JNK or caspase 3 channels alone. The dotted green lines denote clone boundaries. C,J and Q are *z*-section views. Eiger is concentrated at the boundary of Ras^{V12} clones (A-C) but not at the boundary of Ras^{V12}, *sec15* (D,E) or Ras^{V12}, *eiger-RNAi* (F,G) clones. Eiger is moderately retained in *sec15* clones (V,W) but is present at higher levels in Ras^{V12}, *sec15* double mutant clones (D,E). Wild-type cells surrounding Ras^{V12} clones (H-J), but not wild-type cells surrounding Ras^{V12}, *sec15* (K,L) or Ras^{V12}, *eiger-RNAi* (M,N) clones show elevated phospho-JNK levels. Ras^{V12}, *sec15* double mutant clones show elevated phospho-JNK levels (K,L). Correspondingly, cell death can be detected in wild-type cells surrounding Ras^{V12} clones (O-Q) but not in wild-type cells surrounding Ras^{V12}, *sec15* double mutant clones. Instead, cell death is concentrated inside the double mutant clones (R,S). (T,U) Confocal projection showing discs containing Ras^{V12}, *sec15, bsk-DN* triple mutant clones stained with DAPI to mark nuclei and stained for active caspase-3 to detect apoptotic cells. The caspase channel alone is shown in U. (X,Y) *sec15* mutant cells stained with DAPI and anti-phospho-JNK. (Z) Quantification of caspase-positive cells in Ras^{V12} single or Ras^{V12}, *sec15* double or Ras^{V12}, *sec15, bsk-DN* triple mutant clones. Error bars denote standard deviations from the mean for each genotype analyzed. *P* values are derived from a two-tailed distribution with two-sample equal variance *t*-test. Scale bars: 5 µm.

type cells and the resulting JNK activation there, we first blocked Eiger/TNF exocytosis to the surrounding wild-type cells and examined JAK-STAT activation. We found that depleting Eiger/TNF protein specifically in Ras^{V12} cells (Ras^{V12}, *egr-RNAi* clones) or preventing the secretion of Eiger/TNF (Ras^{V12}, *sec15* double mutant cells) or reducing the protein dosage of the Eiger/TNF receptor (Wengen) all suppressed JAK-STAT activity compared to that of Ras^{V12} cells (Fig. 6F; supplementary material Fig. S6E-G). Consistent with these results, wild-type cells surrounding Ras^{V12}, *sec15* double mutant clones failed to up-regulate Upd (supplementary material Fig. S6H). Next, we tested whether directly blocking JNK activation specifically in the surrounding wild-type cells would suppress JAK-STAT activation in Ras^{V12} clones. To prevent JNK activation specifically in wild-type cells surrounding Ras^{V12} clones, we induced Ras^{V12} clones in *JNKKK dtak1* (*Tak1* – FlyBase) mutant discs, but rescued JNKKK/dTAK1 function with a UAS-dTAK1 transgene only in the Ras^{V12} clones (i.e. clones of cells co-expressing Ras^{V12} and *dTAK1* in *dtak1*-null mutant discs). These clones, hereafter referred to as *dtak1//* Ras^{V12} clones, did not show STAT-GFP expression (Fig. 6B), mimicking Ras^{V12}, *egr-RNAi* clones. Finally, we removed the surrounding wild-type cells by expressing Ras^{V12} throughout the developing eye discs [*Eyeless-Gal4>*Ras^{V12}, (*ey>*Ras^{V12})] and examined JAK-STAT activation. These discs did not show broad STAT-GFP induction. Instead, we detected isolated patches of STAT-GFP-positive cells near caspase-positive cells (supplementary material Fig. S6C). Taken together, these findings indicate that it is the activation of JNK signaling specifically in the surrounding wild-type cells that non-cell autonomously stimulates JAK-STAT signaling in Ras^{V12} cells.

JAK-STAT signaling promotes oncogenic Ras-mediated overgrowth

Finally, we sought to investigate whether this Eiger/TNF exocytosis-triggered JNK-JAK-STAT signaling relay contributes to Ras^{V12} tumor growth. If this is the case, then it should be expected that (1) depleting Eiger/TNF in Ras^{V12} cells (Ras^{V12}, *egr-RNAi*), (2)

Development (2014) 141, 4729-4739 doi:10.1242/dev.108092

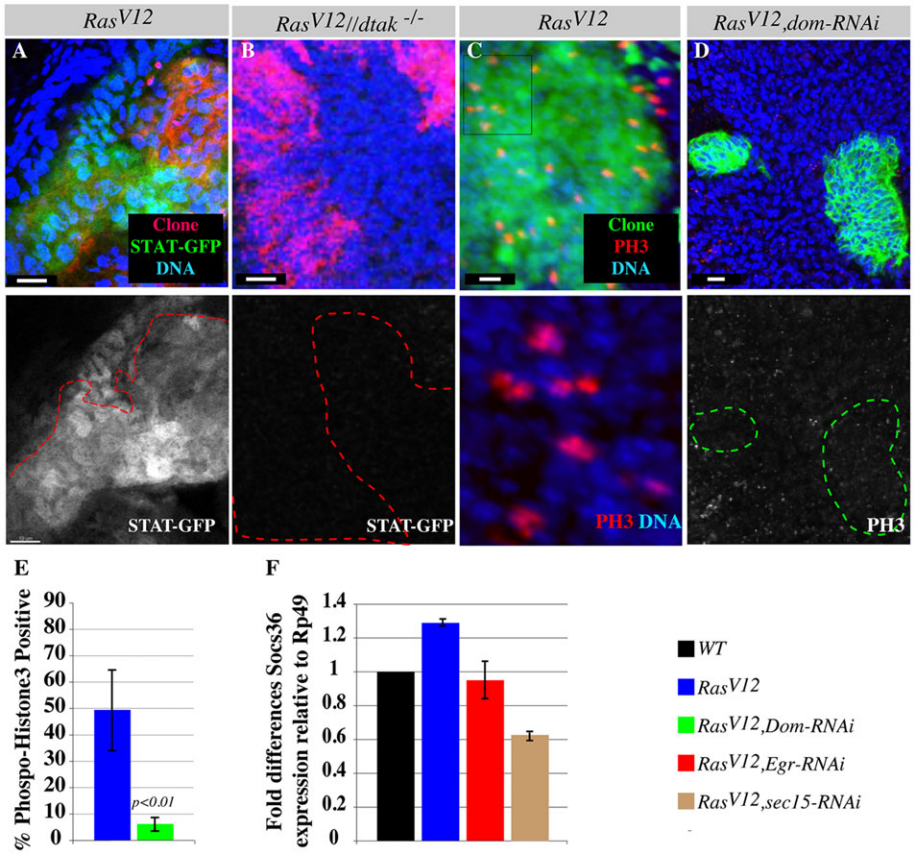

Fig. 6. Eiger/TNF exocytosis activates JAK-STAT signaling through JNK. (A) The JAK-STAT activity GFP-reporter line shows pathway activation in Ras^{V12} clones. The lower panel shows STAT-GFP alone. (B) *dTAK1*-rescued Ras^{V12} clones (red) induced in *dtak1* hemizygous mutant discs do not show JAK-STAT GFP (green) induction. Lower panel shows STAT-GFP alone. The red outlines show clone boundaries in A and B. (C,D) Ras^{V12} or Ras^{V12}, *dom-RNAi* double mutant clones stained with DAPI to mark nuclei and with antibody against the mitotic marker, phospho-histone-3 (PH3). The majority of Ras^{V12} clones are phospho-histone-3 positive (C). The lower panel of C represents a magnified view of DAPI and phospho-histone-3 from the boxed area in the upper panel. Ras^{V12}, *dom-RNAi* clones (D) show reduced phospho-histone-3 staining. The lower panel shows the phospho-histone-3 channel alone. The green outlines show clone boundaries in D. Scale bars: 5 µm. (E) Quantification of C and D. (F) RT-PCR experiment measuring *Socs36E* levels relative to expression levels of the housekeeping gene *Rp49*. Normalized fold differences in *Socs36E* expression levels between Ras^{V12} and wild-type (WT) or between Ras^{V12}, *eiger-RNAi* (*eiger* RNAi-knockdown specifically in *RasV12* clones) and Ras^{V12} or between Ras^{V12}, *sec15* double mutant and Ras^{V12} clones are shown. Experiments were performed in triplicate and standard deviations were derived from the coefficient variations of experimental and control samples.

inducing Ras^{V12} clones in *eiger* mutant animals, (3) directly blocking JNK in wild-type cells surrounding Ras^{V12} cells (Ras^{V12}//*dtak1*, juxtaposed *dtak1* and Ras^{V12} mutant cells) or (4) preventing JAK-STAT activation in Ras^{V12} cells would result in suppression of overgrowth. Indeed, Ras^{V12}, *egr-RNAi* or Ras^{V12} clones induced in *eiger* mutant animals showed reduced growth compared with that of mosaic Ras^{V12} clones (Fig. 7A-C,G). Moreover, Ras^{V12}, *Tace-RNAi* clones, which display no Eiger/TNF accumulation around the clones, showed reduced growth compared with that of Ras^{V12} clones. *Tace-RNAi* alone showed no effect on growth (supplementary material Fig. S3C,G-J). Similarly, Ras^{V12}//*dtak1* mutant cells showed reduced growth compared to that of controls (Fig. 7E-G).

Furthermore, removing the surrounding wild-type cells by expressing Ras^{V12} throughout the eye discs using *eyFLP, Act>y*$^{+}$*>Gal4*, *UAS-*Ras^{V12} or *ey>*Ras^{V12} results only in moderate growth compared to the more pronounced overgrowth of mosaic Ras^{V12} tissues (supplementary material Fig. S6I,J and see figure S1 in Wu et al., 2010). Consistent with reduced growth, *ey>*Ras^{V12} discs do not cause animal lethality, whereas the overgrowth of mosaic Ras^{V12} clones kills the animal during pupal stages (Fig. 1K; supplementary material Fig. S6K). We then tested whether preventing JAK-STAT activation in Ras^{V12} cells, by co-expressing an RNAi transgene against the JAK-STAT receptor, Domeless, (Ras^{V12}, *dom-RNAi* clones) suppresses Ras^{V12} tumor growth. Ras^{V12}, *dom-RNAi* clones showed a reduced mitotic potential as determined by the percentage of phosphorylated-histone-3-positive cells (6.3±5%, *N*=214 for Ras^{V12}, *dom-RNAi* clones and 49.5± 29.5%, *N*=214 for Ras^{V12}; mean±s.d.; Fig. 6C,D,E) and correspondingly showed reduced tumor growth (Fig. 7A,D,G). Similarly, blocking JAK-STAT activity in *ey>*Ras^{V12} (*ey>*Ras^{V12}, *dom-RNAi*) suppresses growth (supplementary material Fig. S5K,L). This suggests that the patches of dying cells contribute to the growth of Ras^{V12} cells. Taken together, the above findings indicate that the accumulation of Eiger/TNF and the resulting activation of JNK signaling in the surrounding wild-type cells non-autonomously promote Ras^{V12} tumor growth through JAK-STAT activation (Fig. 8).

DISCUSSION

Earlier efforts to understand Ras signaling during normal development in model organisms led to the elucidation of the Ras/MAPK signaling cascade (Nishida and Gotoh, 1993; Simon et al., 1991; Sternberg and Horvitz, 1991). However, the signaling events that are elicited by oncogenic Ras to drive overgrowth are complex and not fully understood (reviewed by Mitin et al., 2005). Here, we used a *Drosophila* model and searched for mutations that can block Ras^{V12} overgrowth in an *in vivo* synthetic screen. We identified *sec15*, a mutation in a gene encoding a component of the exocytosis machinery, as a synthetic suppressor of Ras^{V12} tumor growth. Studying the underlying cause of this phenomenon led to the unexpected discovery of both cell-intrinsic and cell-extrinsic mechanisms that promote Ras^{V12} overgrowth.

Oncogenic Ras stimulates Eiger/TNF exocytosis

We found that Ras^{V12} tumors elevate exocytosis to promote rapid clearance of Eiger/TNF and hence avert JNK-mediated cell death. Oncogenic Ras could stimulate the exocyst through the Ral-specific guanine nucleotide exchange factors (RalGEFs). It has been shown that oncogenic Ras activates RalGEFs, which in turn activate the Ras-like small GTPases RalA and RalB (Lim et al., 2005; Urano et al., 1996; White et al., 1996; Wolthuis et al., 1998). Moreover, RalGEF-Ral signaling stimulates gene expression (Neel et al., 2011). It is therefore likely that Ral mediates the observed increased levels of exocyst proteins in Ras^{V12} cells. Consistent with this,

Development (2014) 141, 4729-4739 doi:10.1242/dev.108092

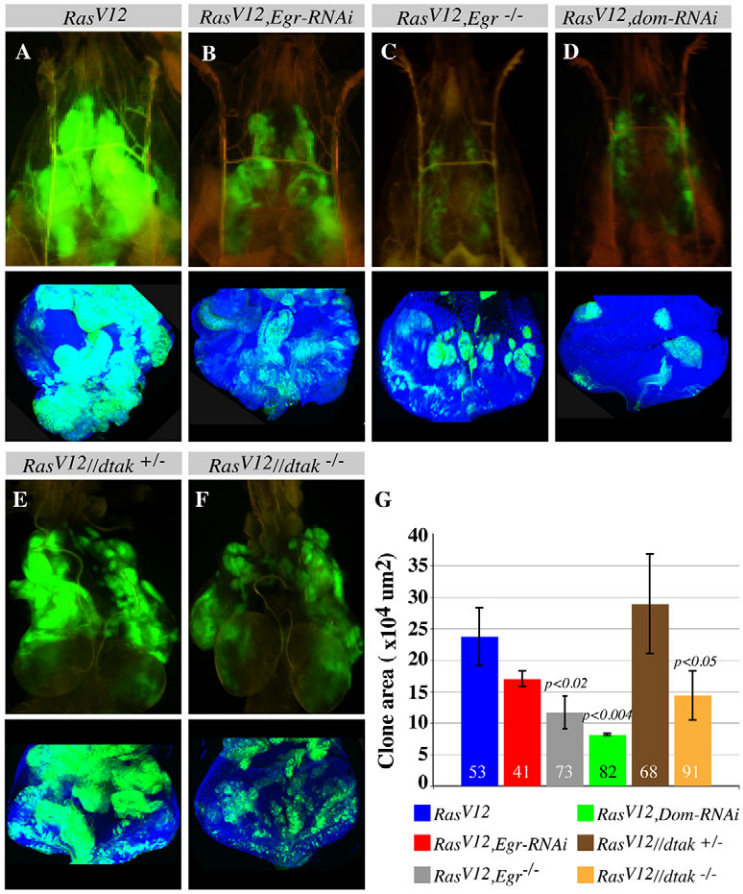

Fig. 7. Eiger/TNF exocytosis activation of JAK-STAT signaling promotes *Ras^{V12}* tumor overgrowth. (A-F) Clones (green) from similarly aged intact third instar larvae (A-D), dissected cephalic regions (E,F) or dissected eye discs (lower panels). *Ras^{V12}* clones overgrow (A). *eiger*/*Tnf* RNAi knockdown specifically in the *Ras^{V12}* clones (B) or generating *Ras^{V12}* clones in *eiger* mutant animals (C) or blocking JAK-STAT signaling by using Domeless RNAi (*dom-RNAi*) (D) suppresses the overgrowth of *Ras^{V12}* clones. Dissected cephalic regions (E,F) or dissected eye discs (lower panels) show that *dTAK1*-rescued *Ras^{V12}* clones induced in *dtak1* hemizygous males (*Ras^{V12}//dtak$^{-/-}$*) (F), exhibit reduced growth compared with *dTAK1*-rescued *Ras^{V12}* clones induced in the siblings (*dtak1* heterozygous females; *Ras^{V12}//dtak$^{+/-}$*) (E). (G) Quantification of A-F. Confocal stacks from similarly aged animals of the indicated genotypes and the image analysis software Imaris were used to measure clone (green) sizes. Error bars show s.d. The numbers in the bars indicate the sample size for the corresponding genotype.

Sec15 transcription is increased in *Ras^{V12}* tissues (supplementary material Fig. S7A). Furthermore, activated Rals interact with and stimulate the exocyst through Exo84 and Sec5 (Hamad et al., 2002; Moskalenko et al., 2002), suggesting that RalGEF-Ral signaling could be the underlying means by which *Ras^{V12}* cells generally stimulate exocytosis. We cannot rule out the possibility that the exocytosis of other molecules is elevated.

Eiger/TNF exocytosis is mediated by the Sec15-Eiger/TNF interaction. Consistent with this, *sec15* mutant cells retain Eiger/TNF. In contrast to *Ras^{V12}*, *sec15* double mutant cells, *sec15* mutant cells do not undergo apoptosis. This is likely owing to the fact that oncogenic Ras stimulates *Eiger*/*TNF* expression (supplementary material Fig. S7B) in addition to promoting Eiger/TNF exocytosis. The Sec15-Eiger/TNF interaction is interesting as it might represent a novel role of the exocyst in cargo selection. It is tempting to speculate that the cytosolic domain of Eiger/TNF could mediate its interaction with the exocyst. In the future it will be interesting to investigate the nature of this interaction, map out the relevant domains and elucidate a sorting mechanism. The finding that oncogenic Ras hijacks the exocytosis machinery to clear up pro-apoptotic ligands provides a new way by which tumor cells can evade cell death and an additional explanation of how exocytosis can modulate signal transduction.

Oncogenic Ras usurps the JNK-JAK-STAT non-autonomous signal to promote overgrowth

We have previously shown that JNK activation triggered by cell polarity defects can stimulate non-autonomous JAK-STAT signaling for proliferation and that JAK-STAT signaling can cooperate with *Ras^{V12}* (Wu et al., 2010). Here, we discovered that one of the effects of oncogenic Ras itself is to hijack this non-autonomous JNK-JAK-STAT proliferation signaling cascade. We propose that Eiger/TNF, including Eiger/TNF from the nearby fast-secreting *Ras^{V12}* cells, is endocytosed but rapidly cleared out of *Ras^{V12}* cells by the exocyst. Elevated exocytosis in *Ras^{V12}* cells creates an imbalance such that the amount of secreted Eiger/TNF is higher than that being internalized. This not only causes a *Ras^{V12}*

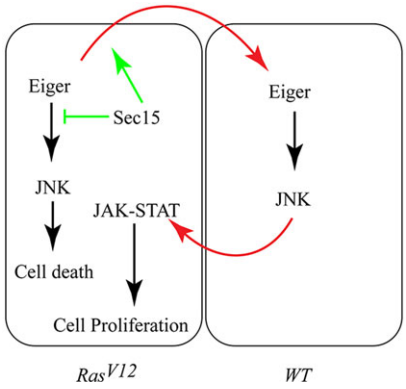

Fig. 8. Oncogenic Ras promotes overgrowth by stimulating Eiger/TNF exocytosis and activating JNK-JAK-STAT non-autonomous proliferation signaling. Eiger normally activates JNK to trigger cell death. JAK-STAT signaling on the other end promotes cell proliferation (black arrows). Sec15 blocks Eiger-induced cell death (green inhibition arrow) by promoting (top green arrow) the exocytosis of Eiger to the surrounding wild-type cells (top red arrow). This results in JNK activation in the surrounding wild-type (WT) cells, which non-autonomously activates the JAK-STAT pathway (bottom red arrow) to promote oncogenic Ras tumor growth.

Development (2014) 141, 4729-4739 doi:10.1242/dev.108092

cell to retain less Eiger/TNF, but the endocytosis and exocytosis cycle also permits neighboring Ras^{V12} cells to relay Eiger/TNF, resulting in the eventual accumulation of Eiger/TNF in the surrounding wild-type cells. Consistent with this, depleting Eiger/TNF or interfering with the exocyst specifically in Ras^{V12} cells abolished Eiger/TNF accumulation around Ras^{V12} clones. Eiger/TNF from Ras^{V12} cells activates JNK signaling in the surrounding wild-type cells. JNK activation stimulates JAK-STAT signaling in Ras^{V12} cells to promote tumor overgrowth. Congruent with this model, JNK activity and the JAK-STAT ligand Upd are upregulated in wild-type cells surrounding Ras^{V12} clones. Preventing Eiger/TNF secretion (Ras^{V12}, *sec15* double mutant clones or Ras^{V12}, *egr*-RNAi clones) suppresses JNK activation, Upd stimulation and JAK-STAT activation in the surrounding wild-type cells. Moreover, blocking JNK signaling specifically in wild-type cells surrounding Ras^{V12} clones prevents JAK-STAT activation in Ras^{V12} cells and suppresses tumor growth.

Interestingly, oncogenic Ras or wound-induced JNK activation does not cause invasion, in contrast to JNK induced by the cell polarity mutation *scrib*. This could be due to context-dependent JNK activation. However, we found that *Sec15-RNAi* suppresses the growth and invasion phenotypes of Ras^{V12}, *scrib* double mutant clones (supplementary material Fig. S8A-D) and rescues animal lethality (supplementary material Fig. S8C-E), highlighting the importance of exocytosis in promoting tumor growth and invasion.

Another striking result of our study is the realization of the importance of the interaction between Ras^{V12} and the surrounding non-Ras^{V12} cells in oncogenic Ras-mediated growth. This is best illustrated by the fact that a tissue in which oncogenic Ras is uniformly expressed grows less than a tissue containing both wild-type and oncogenic Ras-expressing cells. This is consistent with accumulating data from rodents and patients indicating that signaling events emanating from host/stromal cells promote tumor development (Bremnes et al., 2011; Lu et al., 2013; Mueller and Fusenig, 2004; Sounni and Noel, 2012). Additional significance is derived from recent studies of various solid tumors showing heterogeneity within each tumor (Diaz et al., 2012; Gerlinger et al., 2012; Gerstung et al., 2011; Marusyk and Polyak, 2010).

Our study reveals that an important effect of oncogenic Ras is the increased exocytosis of Eiger/TNF. Indeed, the fact that blocking exocytosis of Eiger/TNF can suppress oncogenic Ras-mediated growth highlights the importance of Eiger/TNF exocytosis in cancer biology. Exocytosis proteins are conserved and have been implicated in diverse human cancers types, including Ras cancers (Cheng et al. 2004, 2005; Issaq et al., 2010; Neel et al., 2011; Palmer et al., 2002), suggesting that a similar tumor-promoting mechanism could be at play in vertebrates. Because *sec15* null mutation does not cause cell lethality and the gene is evolutionarily conserved, it suggests a new type of potential therapeutic targets.

MATERIALS AND METHODS

Fly lines

Animals were aged at 25°C on standard medium. The following fly lines were used in this study: (1) *y w; FRT82B*; (2) *y w; FRT82B, UAS-*Ras^{V12}*/TM6B*; (3) *y w; FRT40A, UAS-*Ras^{V12}; (4) *y w; FRT82B, sec15*^{1} (H. Bellen, Baylor College of Medicine, Houston, TX, USA); (5) *y w; UAS-*$RasV^{12}$*; FRT82B, sec15*^{1}*/TM6B*; (6) *UAS-Sec15-RNAi* (VDRC); (7) *FRT40,UAS-*Ras^{V12}*;UAS-eiger-RNAi/TM6B*; (8) *w;UAS-*Ras^{V12}*; FRT82B, Stat92E*^{06346}*/TM6B*; (9) *w;UAS-*Ras^{V12}*; FRT82B,UAS-dom (IR)/TM6B*; (10) *y w,ey-Flp1;act>y+>GAL4,UAS-GFP.S65T;FRT82B,tub-GAL80*; (11) *y w,ey-Flp1;act>y+>GAL4,UAS-myrRFP;FRT82B,tub-GAL80*; (12) *y w,ey-Flp1; tub-GAL80,FRT40A;act>y+>GAL4,UAS-GFP.S65T*; (13) *w;10XSTAT-GFP.1*; (14) *UAS-UAS-BskDN;eyFLP5,Act>y+>Gal4, UAS-GFP/Cyo; FRT82B, Tub-Gal80/TM6B*; (15) *Eyeless-GAL4* (Bloomington); (16) *w, dTak1; ey-Flp5,act>y+>GAL4,UAS-GFP;FRT82B,tub-GAL80*; (17) *w, dTak1; ey-Flp5, act>y+>GAL4,UAS-myrRFP;FRT82B,tub-GAL80*; (18) *UAS-dTAK1; FRT82B, UAS-*Ras^{V12}; (19) *upd-lacZ; UAS-*Ras^{V12}; *sec15*^{1}*, FRT82B/Sb*; (20) *UAS-*Ras^{V12}*, UAS-Sec15-RNAi; 10XSTAT-GFP.1/TM6B*; (21) *ey-FLP5, act>y+>GAL4,UAS-GFP*; (22) *Sec6-RNAi (VDRC)*; (23) *Sec8-RNAi (VDRC)*; (24) *Wgn*^{22} (P. Barker, McGill University, Montreal, Canada); (25) *UAS-TACE-RNAi*; (26) *UAS-TACE*; (27) *UAS-Rab5:GFP* (Bloomington); (28) *GMR-Gal4*; (29) *UAS-Eiger*^{w}; and (30) *UAS-Bsk-DN*.

Staining and imaging

Eye-antenna discs were dissected, fixed and stained as described previously (Igaki et al., 2006; Pagliarini and Xu, 2003; Wu et al., 2010). Tumor and adult eye size analyses were carried out on a Leica MZ FLIII fluorescence stereomicroscope equipped with a camera. Samples were examined by confocal microscopy with a Zeiss LSM510 Meta system. Images were analyzed and processed with Imaris (Bitplane) and Illustrator (Adobe) software, respectively. The following primary antibodies were used: guinea pig anti-Sec6 at 1:1000 [U. Tepass (University of Toronto, Canada) and H. Bellen]; guinea pig anti-Sec8 at 1:1000 (U. Tepass and H. Bellen); guinea pig anti-Sec15 at 1:1000 (H. Bellen); rat anti-Rab11 at 1:1000 (S. Cohen, University of Kansas, USA); rabbit anti-Rab11 at 1:1000 (D. Ready, Purdue University, IN, USA); rabbit anti-Stat92E at 1:1000 (S. Hou); rabbit anti-phospho-histone-3 at 1:1000; rabbit anti-cleaved caspase-3 at 1:500; rabbit anti-Eiger polyclonal antibody R1 at 1:50 (T. Igaki, Kobe University, Japan); mouse anti-phospho-JNK monoclonal antibody G9 at 1:250. Secondary antibodies were from Invitrogen. TUNEL staining was performed using the Apoptag Red kit from Chemicon.

Isosurface rendering

Projections of serial confocal sections were used to generate three-dimensional graphical images using the image analysis software Imaris. The clipping plane function was used to section across the resulting graphical images.

Vesicle trafficking studies

The whole central nervous system, including the attached eye discs, was dissected in Schneider medium and incubated in Schneider medium supplemented with 0.5 mg/ml Dextran-Alexa-546 for 2 h. Half of the samples were immediately washed and fixed. Eye discs were separated and mounted in DAPI-Vectashield. The remaining half of the samples were washed and incubated in Schneider medium for an additional 2 h (chase), rinsed in PBS, fixed and mounted as above.

Western blots and immunoprecipitation

Third instar imaginal discs bearing wild-type or Ras^{V12}-expressing cells were homogenized in lysis buffer (50 mM HEPES pH 7.5, 150 mM KCl, 5 mM $MgCl_2$, supplemented with protease inhibitor tablets; Roche). Samples were separated by SDS-PAGE, transferred onto nitrocellulose membrane and blotted with anti-Sec15, anti-Sec6, anti-Sec8. Lysates were diluted 1:100 and blotted with anti-α-Tubulin antibodies as a loading control. For immunoprecipitation experiments, 500 µl of lysate obtained from discs containing Ras^{V12} clones was pre-cleared with Protein A-agarose beads for 1 h at 4°C, split equally into two tubes and incubated either with 2 µl of anti-Eiger or 2 µl of anti-GFP antibodies for 4 h at 4°C. Lysates were then incubated with Protein A-agarose beads for 1 h at room temperature. For pull downs, beads were precipitated and washed three times in modified lysis buffer containing 0.5% Triton X-100. Samples were separated by SDS-PAGE, transferred onto nitrocellulose membrane and blotted with antibodies against Sec15, Sec8, Sec5 and α-Tubulin.

Real-time polymerase chain reaction

Total RNA from eye-antenna imaginal discs containing wild-type or mutant clones was isolated using a Trizol RNA extraction method. The SuperScript III First-Strand Synthesis System kit was used to synthesize cDNA. Real-time PCR was carried out on an Applied Biosystems machine using the SYBR Green fast kit following the manufacturer's instructions. Relative gene expression was obtained from triplicate runs normalized to *Rp49*

Development (2014) 141, 4729-4739 doi:10.1242/dev.108092

(*RpL32* – FlyBase) as the endogenous control. The following primers were used: *Rp49*, 5′-GGCCCAAGATCGTGAAGAAG-3′ and 5′-ATTTGTGCGACAGCTTAGCATATC-3′; *Socs36E*, 5′-GTCGCTGCCAGTCAGCAA-3′ and 5′-TGCTCCCATTGAAAGTGCTTT-3′; *Sec15*, 5′-CATTATGCTGTCCATCAACACCTT-3′ and 5′-CAGCGTTGCAGTAAAACCTCATT-3′; *eiger*, 5′-GATGGTCTGGATTCCATTGC-3′ and 5′-TAGTCTGCGCCAACATCATC-3′.

Clones of mutant cells in the eye-antennal discs were generated using standard MARCM system (Lee and Luo, 2001) at 25°C. Hanging-eye phenotype experiments were carried out at 29°C. Immunostaining and immunoprecipitation experiments were performed as described previously (Chabu and Doe, 2008; Pagliarini and Xu, 2003).

Acknowledgements

We thank U. Tepass, H. Bellen, D. Ready, S. Cohen and the Vienna Drosophila RNAi Center for kindly providing reagents, and S. Landrette and T. Klein (Yale University, CT, USA) for comments.

Competing interests

The authors declare no competing financial interests.

Author contributions

C.C. and T.X. designed the research, C.C. performed experiments and analyzed the data. C.C. and T.X. wrote the manuscript.

Funding

C.C. is funded by a National Institutes of Health/National Cancer Institute (NIH/NCI) post-doctoral grant [grant number 1F32CA142118-01A1]. This work was also supported by a grant from NIH/NCI to T.X. [R01 CA69408-17] T.X. is a Howard Hughes Medical Institute Investigator. Deposited in PMC for release after 12 months.

Supplementary material

Supplementary material available online at
http://dev.biologists.org/lookup/suppl/doi:10.1242/dev.108092/-/DC1

References

Alessi, D. R., Saito, Y., Campbell, D. G., Cohen, P., Sithanandam, G., Rapp, U., Ashworth, A., Marshall, C. J. and Cowley, S. (1994). Identification of the sites in MAP kinase kinase-1 phosphorylated by p74raf-1. *EMBO J.* **13**, 1610-1619.

Asghar, U., Hawkes, E. and Cunningham, D. (2010). Predictive and prognostic biomarkers for targeted therapy in metastatic colorectal cancer. *Clin. Colorectal Cancer* **9**, 274-281.

Bach, E. A., Ekas, L. A., Ayala-Camargo, A., Flaherty, M. S., Lee, H., Perrimon, N. and Baeg, G.-H. (2007). GFP reporters detect the activation of the Drosophila JAK/STAT pathway in vivo. *Gene Expr. Patterns* **7**, 323-331.

Barbie, D. A., Tamayo, P., Boehm, J. S., Kim, S. Y., Moody, S. E., Dunn, I. F., Schinzel, A. C., Sandy, P., Meylan, E., Scholl, C. et al. (2009). Systematic RNA interference reveals that oncogenic KRAS-driven cancers require TBK1. *Nature* **462**, 108-112.

Black, R. A., Rauch, C. T., Kozlosky, C. J., Peschon, J. J., Slack, J. L., Wolfson, M. F., Castner, B. J., Stocking, K. L., Reddy, P., Srinivasan, S. et al. (1997). A metalloproteinase disintegrin that releases tumour-necrosis factor-alpha from cells. *Nature* **385**, 729-733.

Blobel, C. P. (1997). Metalloprotease-disintegrins: links to cell adhesion and cleavage of TNF alpha and Notch. *Cell* **90**, 589-592.

Blum, R. and Kloog, Y. (2005). Tailoring Ras-pathway–inhibitor combinations for cancer therapy. *Drug Resist. Updat.* **8**, 369-380.

Bos, J. L. (1989). ras oncogenes in human cancer: a review. *Cancer Res.* **49**, 4682-4689.

Brandt, S. M., Dionne, M. S., Khush, R. S., Pham, L. N., Vigdal, T. J. and Schneider, D. S. (2004). Secreted bacterial effectors and host-produced Eiger/TNF drive death in a Salmonella-infected fruit fly. *PLoS Biol.* **2**, e418.

Bremnes, R. M., Al-Shibli, K., Donnem, T., Sirera, R., Al-Saad, S., Andersen, S., Stenvold, H., Camps, C. and Busund, L.-T. (2011). The role of tumor-infiltrating immune cells and chronic inflammation at the tumor site on cancer development, progression, and prognosis: emphasis on non-small cell lung cancer. *J. Thorac. Oncol.* **6**, 824-833.

Chabu, C. and Doe, C. Q. (2008). Dap160/intersectin binds and activates aPKC to regulate cell polarity and cell cycle progression. *Development* **135**, 2739-2746.

Chen, H.-W., Chen, X., Oh, S.-W., Marinissen, M. J., Gutkind, J. S. and Hou, S. X. (2002). mom identifies a receptor for the Drosophila JAK/STAT signal transduction pathway and encodes a protein distantly related to the mammalian cytokine receptor family. *Genes Dev.* **16**, 388-398.

Cheng, K. W., Lahad, J. P., Kuo, W.-L., Lapuk, A., Yamada, K., Auersperg, N., Liu, J., Smith-McCune, K., Lu, K. H., Fishman, D. et al. (2004). The RAB25 small GTPase determines aggressiveness of ovarian and breast cancers. *Nat. Med.* **10**, 1251-1256.

Cheng, K. W., Lahad, J. P., Gray, J. W. and Mills, G. B. (2005). Emerging role of RAB GTPases in cancer and human disease. *Cancer Res.* **65**, 2516-2519.

Chi, C., Zhu, H., Han, M., Zhuang, Y., Wu, X. and Xu, T. (2010). Disruption of lysosome function promotes tumor growth and metastasis in Drosophila. *J. Biol. Chem.* **285**, 21817-21823.

Cordero, J. B., Macagno, J. P., Stefanatos, R. K., Strathdee, K. E., Cagan, R. L. and Vidal, M. (2010). Oncogenic Ras diverts a host TNF tumor suppressor activity into tumor promoter. *Dev. Cell* **18**, 999-1011.

Cowley, S., Paterson, H., Kemp, P. and Marshall, C. J. (1994). Activation of MAP kinase kinase is necessary and sufficient for PC12 differentiation and for transformation of NIH 3T3 cells. *Cell* **77**, 841-852.

Cox, A. D. and Der, C. J. (2003). The dark side of Ras: regulation of apoptosis. *Oncogene* **22**, 8999-9006.

Diaz, L. A., Jr, Williams, R. T., Wu, J., Kinde, I., Hecht, J. R., Berlin, J., Allen, B., Bozic, I., Reiter, J. G., Nowak, M. A. (2012). The molecular evolution of acquired resistance to targeted EGFR blockade in colorectal cancers. *Nature* **486**, 537-540.

Dollar, G., Struckhoff, E., Michaud, J. and Cohen, R. S. (2002). Rab11 polarization of the Drosophila oocyte: a novel link between membrane trafficking, microtubule organization, and oskar mRNA localization and translation. *Development* **129**, 517-526.

Downward, J. (1998). Ras signalling and apoptosis. *Curr. Opin. Genet. Dev.* **8**, 49-54.

Finger, F. P. and Novick, P. (1998). Spatial regulation of exocytosis: lessons from yeast. *J. Cell Biol.* **142**, 609-612.

Finger, F. P., Hughes, T. E. and Novick, P. (1998). Sec3p is a spatial landmark for polarized secretion in budding yeast. *Cell* **92**, 559-571.

Gerlinger, M., Rowan, A. J., Horswell, S., Larkin, J., Endesfelder, D., Gronroos, E., Martinez, P., Matthews, N., Stewart, A., Tarpey, P. et al. (2012). Intratumor heterogeneity and branched evolution revealed by multiregion sequencing. *N. Engl. J. Med.* **366**, 883-892.

Gerstung, M., Eriksson, N., Lin, J., Vogelstein, B. and Beerenwinkel, N. (2011). The temporal order of genetic and pathway alterations in tumorigenesis. *PLoS ONE* **6**, e27136.

Grindstaff, K. K., Yeaman, C., Anandasabapathy, N., Hsu, S.-C., Rodriguez-Boulan, E., Scheller, R. H. and Nelson, W. J. (1998). Sec6/8 complex is recruited to cell-cell contacts and specifies transport vesicle delivery to the basal-lateral membrane in epithelial cells. *Cell* **93**, 731-740.

Guo, W., Grant, A. and Novick, P. (1999). Exo84p is an exocyst protein essential for secretion. *J. Biol. Chem.* **274**, 23558-23564.

Hamad, N. M., Elconin, J. H., Karnoub, A. E., Bai, W., Rich, J. N., Abraham, R. T., Der, C. J. and Counter, C. M. (2002). Distinct requirements for Ras oncogenesis in human versus mouse cells. *Genes Dev.* **16**, 2045-2057.

Heider, M. R. and Munson, M. (2012). Exorcising the exocyst complex. *Traffic* **13**, 898-907.

Igaki, T., Pagliarini, R. A. and Xu, T. (2006). Loss of cell polarity drives tumor growth and invasion through JNK activation in Drosophila. *Curr. Biol.* **16**, 1139-1146.

Igaki, T., Pastor-Pareja, J. C., Aonuma, H., Miura, M. and Xu, T. (2009). Intrinsic tumor suppression and epithelial maintenance by endocytic activation of Eiger/TNF signaling in Drosophila. *Dev. Cell* **16**, 458-465.

Issaq, S. H., Lim, K.-H. and Counter, C. M. (2010). Sec5 and Exo84 foster oncogenic ras-mediated tumorigenesis. *Mol. Cancer Res.* **8**, 223-231.

Jafar-Nejad, H., Andrews, H. K., Acar, M., Bayat, V., Wirtz-Peitz, F., Mehta, S. Q., Knoblich, J. A. and Bellen, H. J. (2005). Sec15, a component of the exocyst, promotes notch signaling during the asymmetric division of Drosophila sensory organ precursors. *Dev. Cell* **9**, 351-363.

Johansen, K. A., Iwaki, D. D. and Lengyel, J. A. (2003). Localized JAK/STAT signaling is required for oriented cell rearrangement in a tubular epithelium. *Development* **130**, 135-145.

Jue, D. M., Sherry, B., Luedke, C., Manogue, K. R. and Cerami, A. (1990). Processing of newly synthesized cachectin/tumor necrosis factor in endotoxin-stimulated macrophages. *Biochemistry* **29**, 8371-8377.

Karim, F. D. and Rubin, G. M. (1998). Ectopic expression of activated Ras1 induces hyperplastic growth and increased cell death in Drosophila imaginal tissues. *Development* **125**, 1-9.

Karsten, P., Häder, S. and Zeidler, M. P. (2002). Cloning and expression of Drosophila SOCS36E and its potential regulation by the JAK/STAT pathway. *Mech. Dev.* **117**, 343-346.

Kauppila, S., Maaty, W. S. A., Chen, P., Tomar, R. S., Eby, M. T., Chapo, J., Chew, S., Rathore, N., Zachariah, S., Sinha, S. K. et al. (2003). Eiger and its receptor, Wengen, comprise a TNF-like system in Drosophila. *Oncogene* **22**, 4860-4867.

Kolch, W., Heidecker, G., Lloyd, P. and Rapp, U. R. (1991). Raf-1 protein kinase is required for growth of induced NIH/3T3 cells. *Nature* **349**, 426-428.

Lee, T. and Luo, L. (2001). Mosaic analysis with a repressible cell marker (MARCM) for Drosophila neural development. *Trends Neurosci.* **24**, 251-254.
Li, L. and Chin, L. S. (2003). The molecular machinery of synaptic vesicle exocytosis. *Cell. Mol. Life Sci.* **60**, 942-960.
Lièvre, A., Blons, H. and Laurent-Puig, P. (2010). Oncogenic mutations as predictive factors in colorectal cancer. *Oncogene* **29**, 3033-3043.
Lim, K.-H., Baines, A. T., Fiordalisi, J. J., Shipitsin, M., Feig, L. A., Cox, A. D., Der, C. J. and Counter, C. M. (2005). Activation of RalA is critical for Ras-induced tumorigenesis of human cells. *Cancer Cell* **7**, 533-545.
Lu, J., Ye, X., Fan, F., Xia, L., Bhattacharya, R., Bellister, S., Tozzi, F., Sceusi, E., Zhou, Y., Tachibana, I. et al. (2013). Endothelial cells promote the colorectal cancer stem cell phenotype through a soluble form of jagged-1. *Cancer Cell* **23**, 171–185.
Luo, J., Emanuele, M. J., Li, D., Creighton, C. J., Schlabach, M. R., Westbrook, T. F., Wong, K.-K. and Elledge, S. J. (2009). A genome-wide RNAi screen identifies multiple synthetic lethal interactions with the Ras oncogene. *Cell* **137**, 835-848.
Mansour, S. J., Matten, W. T., Hermann, A. S., Candia, J. M., Rong, S., Fukasawa, K., Vande Woude, G. F. and Ahn, N. G. (1994). Transformation of mammalian cells by constitutively active MAP kinase kinase. *Science* **265**, 966-970.
Marusyk, A. and Polyak, K. (2010). Tumor heterogeneity: causes and consequences. *Biochim. Biophys. Acta* **1805**, 105-117.
Mehta, S. Q., Hiesinger, P. R., Beronja, S., Zhai, R. G., Schulze, K. L., Verstreken, P., Cao, Y., Zhou, Y., Tepass, U., Crair, M. C. et al. (2005). Mutations in Drosophila sec15 reveal a function in neuronal targeting for a subset of exocyst components. *Neuron* **46**, 219-232.
Mitin, N., Rossman, K. L. and Der, C. J. (2005). Signaling interplay in Ras superfamily function. *Curr. Biol.* **15**, R563.
Moreno, E., Yan, M. and Basler, K. (2002). Evolution of TNF signaling mechanisms: JNK-dependent apoptosis triggered by Eiger, the Drosophila homolog of the TNF superfamily. *Curr. Biol.* **12**, 1263-1268.
Moskalenko, S., Henry, D. O., Rosse, C., Mirey, G., Camonis, J. H. and White, M. A. (2002). The exocyst is a Ral effector complex. *Nat. Cell Biol.* **4**, 66-72.
Moss, M. L., Jin, S.-L., Milla, M. E., Burkhart, W., Carter, H. L., Chen, W.-J., Clay, W. C., Didsbury, J. R., Hassler, D., Hoffman, C. R. et al. (1997). Cloning of a disintegrin metalloproteinase that processes precursor tumour-necrosis factor-alpha. *Nature* **385**, 733-736.
Mueller, M. M. and Fusenig, N. E. (2004). Friends or foes - bipolar effects of the tumour stroma in cancer. *Nat. Rev. Cancer* **4**, 839-849.
Narasimamurthy, R., Geuking, P., Ingold, K., Willen, L., Schneider, P. and Basler, K. (2009). Structure-function analysis of Eiger, the Drosophila TNF homolog. *Cell Res.* **19**, 392-394.
Neel, N. F., Martin, T. D., Stratford, J. K., Zand, T. P., Reiner, D. J., Der, C. J. (2011). The RalGEF-Ral effector signaling network: the road less traveled for anti-ras drug discovery. *Genes Cancer* **2**, 275-287.
Nishida, E. and Gotoh, Y. (1993). The MAP kinase cascade is essential for diverse signal transduction pathways. *Trends Biochem. Sci.* **18**, 128-131.
Novick, P., Field, C. and Schekman, R. (1980). Identification of 23 complementation groups required for post-translational events in the yeast secretory pathway. *Cell* **21**, 205-215.
Pagliarini, R. A. and Xu, T. (2003). A genetic screen in Drosophila for metastatic behavior. *Science* **302**, 1227-1231.
Palmer, R. E., Lee, S. B., Wong, J. C., Reynolds, P. A., Zhang, H., Truong, V., Oliner, J. D., Gerald, W. L. and Haber, D. A. (2002). Induction of BAIAP3 by the EWS-WT1 chimeric fusion implicates regulated exocytosis in tumorigenesis. *Cancer Cell* **2**, 497-505.
Pérez-Garijo, A., Fuchs, Y. and Steller, H. (2013). Apoptotic cells can induce non-autonomous apoptosis through the TNF pathway. *Elife* **2**, e01004.
Qiu, R.-G., Chen, J., Kirn, D., McCormick, F. and Symons, M. (1995). An essential role for Rac in Ras transformation. *Nature* **374**, 457-459.
Ryoo, H. D., Gorenc, T. and Steller, H. (2004). Apoptotic cells can induce compensatory cell proliferation through the JNK and the Wingless signaling pathways. *Dev. Cell* **7**, 491-501.
Sarthy, A. V., Morgan-Lappe, S. E., Zakula, D., Vernetti, L., Schurdak, M., Packer, J. C. L., Anderson, M. G., Shirasawa, S., Sasazuki, T. and Fesik, S. W. (2007). Survivin depletion preferentially reduces the survival of activated K-Ras-transformed cells. *Mol. Cancer Ther.* **6**, 269-276.
Scholl, C., Fröhling, S., Dunn, I. F., Schinzel, A. C., Barbie, D. A., Kim, S. Y., Silver, S. J., Tamayo, P., Wadlow, R. C., Ramaswamy, S. et al. (2009). Synthetic lethal interaction between oncogenic KRAS dependency and STK33 suppression in human cancer cells. *Cell* **137**, 821-834.
Seto, E. S., Bellen, H. J. and Lloyd, T. E. (2002). When cell biology meets development: endocytic regulation of signaling pathways. *Genes Dev.* **16**, 1314-1336.
Simon, M. A., Bowtell, D. D. L., Dodson, G. S., Laverty, T. R. and Rubin, G. M. (1991). Ras1 and a putative guanine nucleotide exchange factor perform crucial steps in signaling by the sevenless protein tyrosine kinase. *Cell* **67**, 701-716.
Sonnichsen, B., De Renzis, S., Nielsen, E., Rietdorf, J. and Zerial, M. (2000). Distinct membrane domains on endosomes in the recycling pathway visualized by multicolor imaging of Rab4, Rab5, and Rab11. *J. Cell Biol.* **149**, 901-914.
Sounni, N. E. and Noel, A. (2012). Targeting the tumor microenvironment for cancer therapy. *Clin. Chem.* **59**, 85-93.
Steckel, M., Molina-Arcas, M., Weigelt, B., Marani, M., Warne, P. H., Kuznetsov, H., Kelly, G., Saunders, B., Howell, M., Downward, J. et al. (2012). Determination of synthetic lethal interactions in KRAS oncogene-dependent cancer cells reveals novel therapeutic targeting strategies. *Cell Res.* **22**, 1227-1245.
Sternberg, P. W. and Horvitz, H. R. (1991). Signal transduction during C. elegans vulval induction. *Trends Genet.* **7**, 366-371.
Strebhardt, K. and Ullrich, A. (2006). Targeting polo-like kinase 1 for cancer therapy. *Nat. Rev. Cancer* **6**, 321-330.
Sun, Y. H., Tsai, C. J., Green, M. M., Chao, J. L., Yu, C. T., Jaw, T. J., Yeh, J. Y. and Bolshakov, V. N. (1995). White as a reporter gene to detect transcriptional silencers specifying position-specific gene expression during Drosophila melanogaster eye development. *Genetics* **141**, 1075-1086.
TerBush, D. R. and Novick, P. (1995). Sec6, Sec8, and Sec15 are components of a multisubunit complex which localizes to small bud tips in Saccharomyces cerevisiae. *J. Cell Biol.* **130**, 299-312.
Ullrich, O., Reinsch, S., Urbe, S., Zerial, M. and Parton, R. G. (1996). Rab11 regulates recycling through the pericentriolar recycling endosome. *J. Cell Biol.* **135**, 913-924.
Urano, T., Emkey, R. and Feig, L. A. (1996). Ral-GTPases mediate a distinct downstream signaling pathway from Ras that facilitates cellular transformation. *EMBO J.* **15**, 810-816.
White, M. A., Vale, T., Camonis, J. H., Schaefer, E. and Wigler, M. H. (1996). A role for the Ral guanine nucleotide dissociation stimulator in mediating Ras-induced transformation. *J. Biol. Chem.* **271**, 16439-16442.
Wolfman, J. C., Palmby, T., Der, C. J. and Wolfman, A. (2002). Cellular N-Ras promotes cell survival by downregulation of Jun N-terminal protein kinase and p38. *Mol. Cell. Biol.* **22**, 1589-1606.
Wolthuis, R. M. F., Zwartkruis, F., Moen, T. C. and Bos, J. L. (1998). Ras-dependent activation of the small GTPase Ral. *Curr. Biol.* **8**, 471-474.
Wu, S., Mehta, S. Q., Pichaud, F., Bellen, H. J. and Quiocho, F. A. (2005). Sec15 interacts with Rab11 via a novel domain and affects Rab11 localization in vivo. *Nat. Struct. Mol. Biol.* **12**, 879-885.
Wu, Y., Zhuang, Y., Han, M., Xu, T. and Deng, K. (2009). Ras promotes cell survival by antagonizing both JNK and Hid signals in the Drosophila eye. *BMC Dev. Biol.* **9**, 53.
Wu, M., Pastor-Pareja, J. C. and Xu, T. (2010). Interaction between RasV12 and scribbled clones induces tumour growth and invasion. *Nature* **463**, 545-548.
Zhang, X.-M., Ellis, S., Sriratana, A., Mitchell, C. A. and Rowe, T. (2004). Sec15 is an effector for the Rab11 GTPase in mammalian cells. *J. Biol. Chem.* **279**, 43027-43034.